iScience

CellPress
OPEN ACCESS

Article

Resistin targets TAZ to promote osteogenic differentiation through PI3K/AKT/mTOR pathway

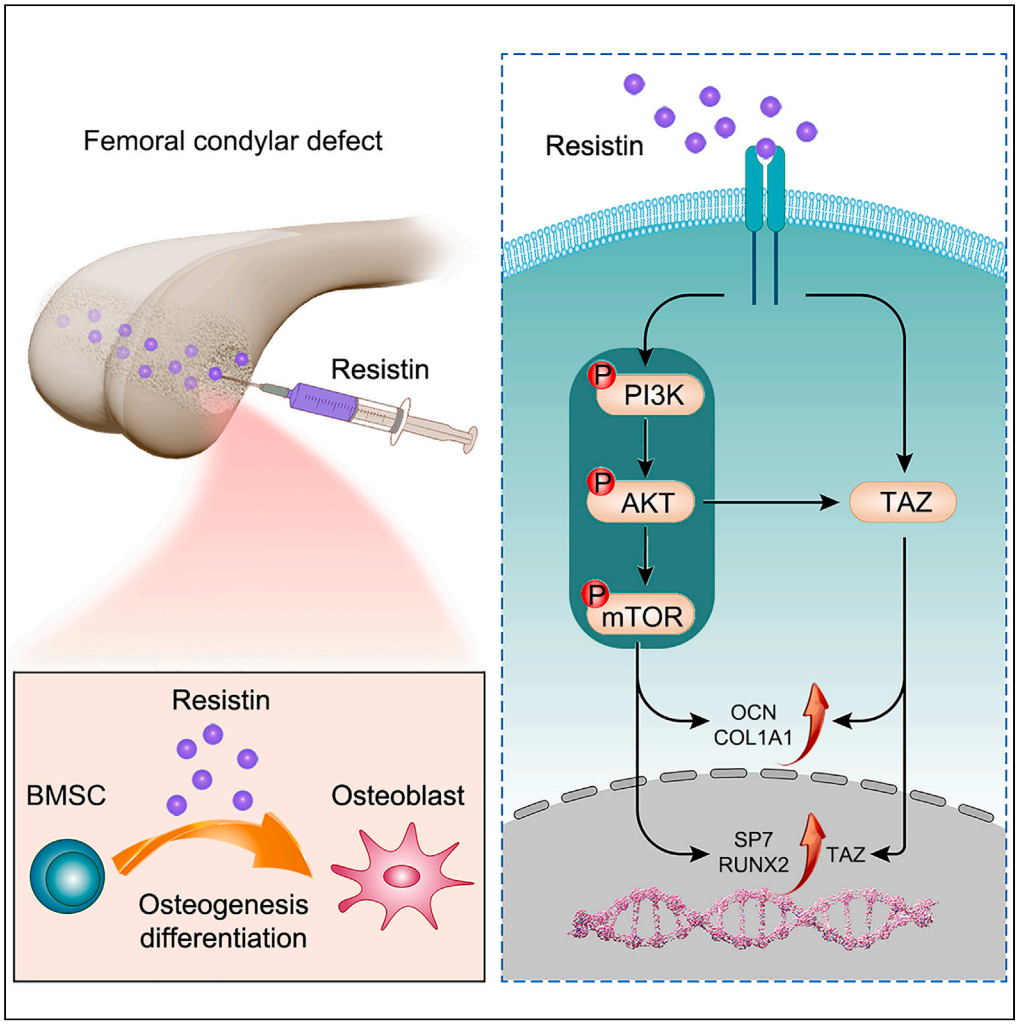

JingJing Shang, Zhentang Yu, Chengwei Xiong, ..., Changlin Yu, Yong Huang, Xindie Zhou

xindiezhou@163.com

Highlights

Resistin is expressed at a higher level in the BMSCs OD process

Upregulation of resistin significantly promotes OD of BMSCs

Resistin regulates OD via PI3K/AKT/mTOR pathway

Resistin targets TAZ to promote OD of BMSCs

Shang et al., iScience *26*, 107025
July 21, 2023
https://doi.org/10.1016/j.isci.2023.107025

iScience

CellPress
OPEN ACCESS

Article

Resistin targets TAZ to promote osteogenic differentiation through PI3K/AKT/mTOR pathway

JingJing Shang,[1,3,6] Zhentang Yu,[2,3,4,6] Chengwei Xiong,[2,3] Junjie Zhang,[2,3] Jinhong Gong,[1,3] Changlin Yu,[2,3] Yong Huang,[2,3] and Xindie Zhou[2,3,5,7,*]

SUMMARY

Osteogenic differentiation (OD) of bone marrow mesenchymal stem cells (BMSCs) contributes significantly to the regeneration of bone defects. Resistin, an adipose tissue-specific secretory factor, has been shown to involve many different functions, including metabolism, inflammation, cancer, and bone remodeling. However, the effects and mechanisms of resistin on OD of BMSCs remain unclear. Herein, we demonstrated that resistin was highly expressed in BMSCs with OD. Upregulation of resistin contributed to the progression of OD of BMSCs by activating PI3K/AKT/mTOR signaling pathway. In addition, resistin facilitated OD by targeting transcriptional co-activator with PDZ-binding motif (TAZ). In a rat femoral condyle bone defect model, local injection of resistin significantly promoted bone repair and improved bone formation. This work contributes to better understanding the mechanism of resistin directly involved in the OD and might provide a new therapeutic strategy for bone defect regeneration.

INTRODUCTION

Bone tissue engineering continues to explore a strategy to enhance the regeneration of bone defects, but repair remains a substantial challenge for modern medicine.[1,2] Bone defects can be caused by various disorders, including trauma, tumors, infections, congenital malformation, and other diseases. Severe bone defects usually lead to disability, reduced quality of life, and ability to work, and a severe burden on society and the economy. Currently, more than 100,000 patients suffer delayed union or non-union traumatic fractures every year in the US, which costs an estimated 1.2 billion annually.[3] Existing treatment modalities for bone defects are based on autografts, allografts, and bone grafts substitutes. Unfortunately, clinical application is limited because of insufficient autologous bone, supply source limitations, and a high rate of immune rejection. The combination based on bone marrow mesenchymal stem cells (BMSCs), scaffolds, and growth factors has proven to be a promising strategy for regenerative therapies of bone defects.[4,5]

BMSCs, located primarily in the bone marrow cavity, are multipotent stem cells with the potential for self-renewal and multidirectional differentiation. Under certain conditions, BMSCs can differentiate into multiple cell types, including adipocytes, chondrocytes, myoblasts, and osteoblasts.[6,7] Moreover, they have been used extensively in studies related to acute myocardial infarction, osteogenesis imperfecta, and tissue repair.[8–10] Owing to the unique characteristics of multiple differentiation, they can repair damaged and degraded skeletal tissue by transplantation. Therefore, exploring the main factors of osteogenic differentiation (OD) will undoubtedly lead to a new strategy for treating bone defects. Accumulating evidence suggests that the PI3K/AKT signaling pathway, a critical player in regulating the functions of osteoblasts and osteoclasts, is vital in maintaining the dynamic balance in bone remodeling.[11–13] Similarly, as a transcriptional co-activator in the Hippo signaling pathway, transcriptional co-activator with Tafazzin (TAZ) can regulate the balance between adipogenic and osteogenic differentiation of BMSCs.[14,15]

Resistin, an adipose tissue-specific secretory factor, belongs to the family of resistin-like molecules (RELMs) and is expressed in humans by many cells, including adipocytes, peripheral blood mononuclear cells, macrophages, and bone marrow cells.[16] It has been reported that resistin may participate in physiological and pathological processes, including metabolism, inflammation, cancer, and bone remodeling.[17–20] However, the effects and mechanisms of resistin on OD of BMSCs remain unclear. Previous studies have revealed that resistin induces cell proliferation, promotes angiogenesis, and reduces insulin sensitivity through PI3K/AKT

[1]Department of Pharmacy, The Affiliated Changzhou Second People's Hospital of Nanjing Medical University, Changzhou, Jiangsu 213000, China

[2]Department of Orthopedics, The Affiliated Changzhou Second People's Hospital of Nanjing Medical University, Changzhou, Jiangsu 213000, China

[3]Changzhou Medical Center, Nanjing Medical University, Changzhou, Jiangsu 213000, China

[4]Department of Graduate School, Dalian Medical University, Dalian, Liaoning 116000, China

[5]Department of Orthopedics, Gonghe County Hospital of Traditional Chinese Medicine, Hainan Tibetan Autonomous Prefecture, Qinghai 811800, China

[6]These authors contributed equally

[7]Lead contact

*Correspondence: xindiezhou@163.com

https://doi.org/10.1016/j.isci.2023.107025

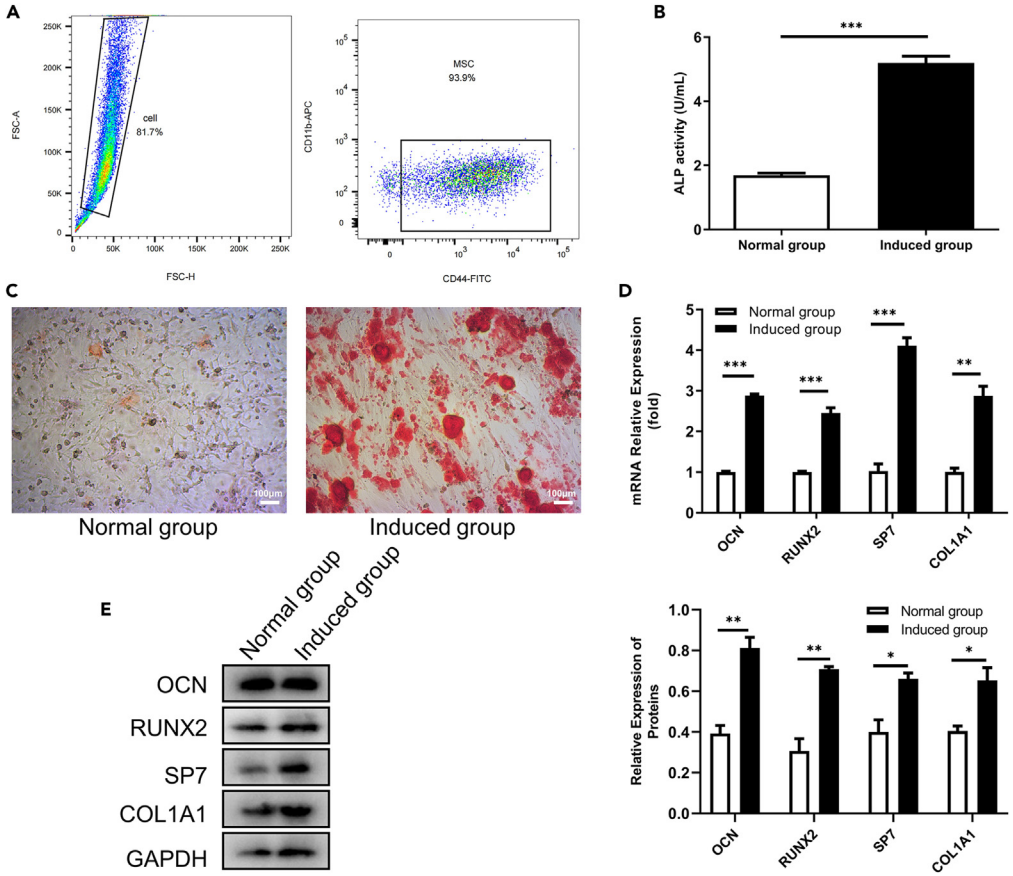

Figure 1. Identification and characteristics of BMSCs

(A) Characterization of BMSCs surface antigens by flow cytometry.

(B) Osteogenic activity evaluated by ALP activity assay.

(C) Calcium deposition visualized by alizarin red staining (scale bar, 100μm).

(D) Relative mRNA levels of OD-related genes (RUNX2, OCN, SP7, and COL1A1).

(E) Relative expression levels of OD related proteins (RUNX2, OCN, SP7, and COL1A1). Densitometry was performed using ImageJ software. Data were presented as means ± SEM. (*$p < 0.05$, **$p < 0.01$, and ***$p < 0.001$, Student's *t* test).

signaling pathway.[21–23] Moreover, recent studies have shown that TAZ regulates the expression and secretion of resistin in mature adipocytes.[19]

Thus, we hypothesized that resistin might regulate the OD of BMSCs by TAZ and PI3K/AKT/mTOR pathways. Exploring exact molecular regulatory mechanisms involved in the OD of BMSCs might provide clues on new treatments and drug development for bone defect regeneration.

RESULTS

Identification and characteristics of rat BMSCs

BMSCs were isolated from rat femurs and cultured *in vitro*. After BMSCs at passage 3 reached 80–90% confluency, immunophenotypes of BMSCs were detected using flow cytometry. As shown in Figure 1A, the expression of CD44 was positive on BMSCs, whereas CD11b was negative. BMSCs were divided into two groups, one group was replaced with an osteogenic differentiation medium, and the other was continued cultured with the initial medium. ALP activity was an early marker in the OD of BMSCs. Furthermore, osteogenic-induced BMSCs showed higher osteogenic capability than the normal group (Figure 1B). In addition, Alizarin red staining was performed to assay the calcified nodule formation, and the osteogenic induction group showed more apparent mineral deposition (Figure 1C). These results indicated that BMSCs were isolated and cultured successfully for subsequent experiments.

Recent studies revealed that RUNX2, OCN, SP7, and COL1A1 were closely related to multiple steps of OD of BMSCs.[24,25] Accordingly, we studied the expression pattern of these genes in greater detail to explore the OD of BMSCs. As shown in Figure 1D, the mRNA expression of RUNX2, OCN, SP7, and COL1A1 was significantly increased in the induced group compared with the normal group. Western blot analysis further confirmed these results (Figure 1E).

Resistin significantly promotes osteogenic differentiation

As mentioned earlier, resistin played a critical role in many human diseases through PI3K/AKT/mTOR pathway.[21–23] PI3K/AKT/mTOR pathway is essential in regulating OD.[11–13] Thus, resistin might also be involved in the regulation of the osteogenesis process. qRT-PCR analysis revealed that the mRNA expression of resistin was obviously increased in the induced group compared to the normal group (Figure 2A). Western blot confirmed the result at the protein level (Figure 2B).

To explore the function of resistin toward OD, 10 ng/ml resistin was added to the osteogenic induction medium. Cells were allowed to grow for 14 days, and adverse events were checked every 7 days. Consistent with our hypothesis, the expression of RUNX2, OCN and COL1A1 was significantly increased in the induced + resistin group compared with the induced group at the mRNA and protein level, and the difference at day 14 was more significant (Figures 2C and 2D).

Resistin promotes OD through the activation of the PI3K/AKT/mTOR pathway

As BMSCs with OD expressed higher levels of resistin than normal control, we proposed that resistin overexpressing promoted OD of BMSCs *in vitro*. Then, we constructed si-resistin and pcDNA3.1-resistin to down-regulated and up-regulated resistin, respectively (Figure 3A). The related events were observed weekly for the next 2 weeks. Consistent with our hypothesis, overexpression of resistin significantly increased the gene expression of OD markers OCN and COL1A1. Moreover, by day 14 more significant difference was observed (Figure 3B). As illustrated in Figure 3C, significant upregulation of p-PI3K and p-AKT suggested the activation of related signaling pathways. Furthermore, the protein expression of p-PI3K, p-AKT, and p-mTOR were significantly increased after resistin treatment (Figure 3D). To further investigate the exact relationships between resistin and PI3K/AKT/mTOR, we co-transfected uprosertib (AKT inhibitor) with pcDNA3.1-resistin. Then, we found that the blockade of the PI3K/AKT/mTOR pathway significantly reversed the impact of resistin overexpression (Figure 3B). This contrast became more pronounced at day 14 (Figure 3B).

Immunofluorescence staining was performed further to confirm the effect of resistin on the OD of BMSCs. This result revealed that RUNX2 expression in the nucleus was significantly lower in the si-Resistin group than in the si-NC group (Figures 4A and 4B). Moreover, we found higher RUNX2 expression in the pcDNA3.1-Resistin group compared to the control and pcDNA3.1 groups (Figures 4A and 4B). In this way, overexpression of resistin promoted OD of BMSCs, and the downregulation of resistin inhibited this process. Again, immunofluorescence staining showed that with the addition of uprosertib, the ratio of RUNX2-positive cells to DAPI-positive cells was decreased compared with the pcdna3.1-Resistin group (Figures 4A and 4B). We concluded that up-regulated resistin facilitated OD of BMSCs via activating PI3K/AKT/mTOR pathway.

Resistin targets TAZ to promote OD of BMSCs

Recent studies revealed a strong correlation between resistin and TAZ, and TAZ/resistin was a potential chemotherapeutic target for breast cancer.[19] Western blot results showed significantly up-regulated TAZ expression in the induced group (Figure 5A). To further study the detailed mechanism of resistin in supporting OD of BMSCs, we assessed the differential expression of TAZ protein after resistin treatment. Subsequently, we found that the TAZ mRNA expression was significantly increased after the intervention (Figure 5B), and Western blot analysis confirmed this change (Figure 5C). Of interest, the AKT inhibitor treatment blocked resistin induced upregulation of TAZ. And the levels of TAZ in pcDNA3.1-Resistin+-uprosertib were increased compared with si-Resistin, suggesting PI3K/AKT/mTOR negatively controls resistin-TAZ signaling axis (Figure 5D). Next, we further explored the relationship between TAZ and PI3K/AKT/mTOR pathway, and the result showed that activation of PI3K/AKT/mTOR pathway increased TAZ expression, in contrast, inhibition of PI3K/AKT/mTOR pathway decreased TAZ expression (Figure 5E). This indicates that resistin promotes TAZ expression to promote OD by activating the PI3K/AKT/mTOR pathway.

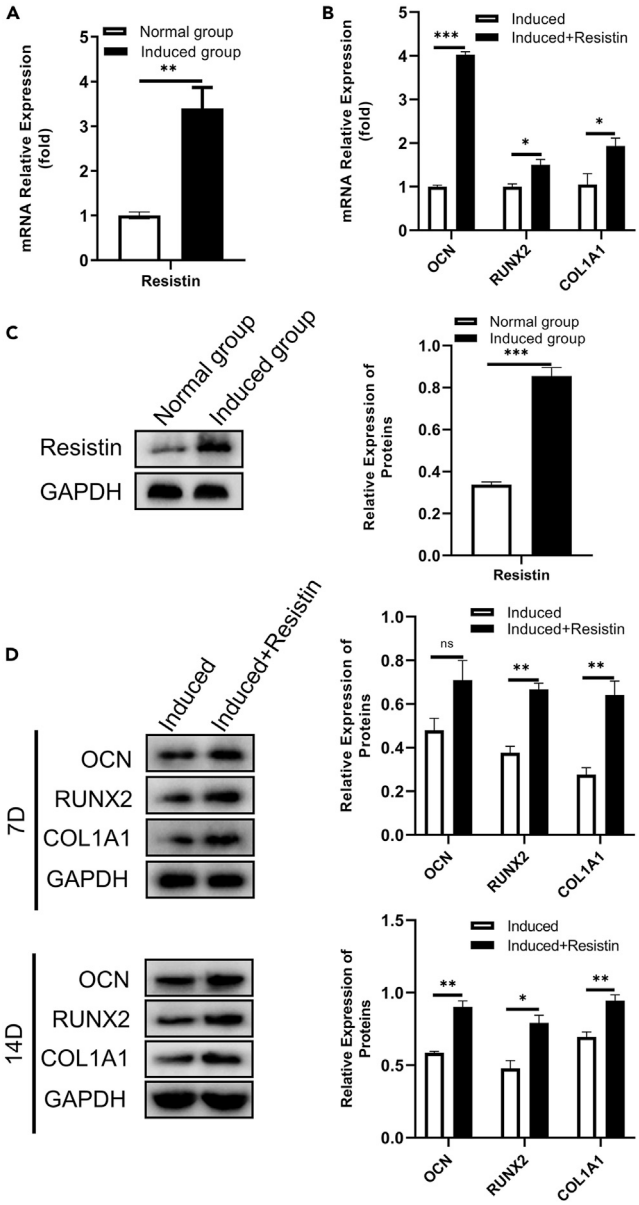

Figure 2. Resistin significantly promotes OD

(A) Relative mRNA levels of resistin.

(B) Relative protein levels of resistin.

(C) Resistin significantly increased the mRNA expression of OD-related genes RUNX2, OCN, and COL1A1.

(D) Resistin significantly increased the expression of OD-related proteins (RUNX2, OCN, and COL1A1) at day 7 and 14. Densitometry was performed using ImageJ software. Data were presented as means ± SEM. (*$p < 0.05$, **$p < 0.01$, and ***$p < 0.001$, Student's *t* test).

Then, TAZ knockdown was obtained by transfecting with si-TAZ plasmid. Furthermore, si-TAZ counteracted the up-regulation of osteogenic markers (RUNX2, OCN, and COL1A1) induced by resistin (Figure 5F). Collectively, these data demonstrated an underlying gene regulatory network in the regulation of BMSCs, and resistin might promote OD via targeting TAZ.

Resistin enhances bone healing of femoral condyle defect

Rats received an equal volume (1 mL) of 0.9% saline or exogenous resistin (10 ng/mL) in the area with femoral condyle defect via intraperitoneal injection once a week. After 4 weeks, femoral condyle specimens

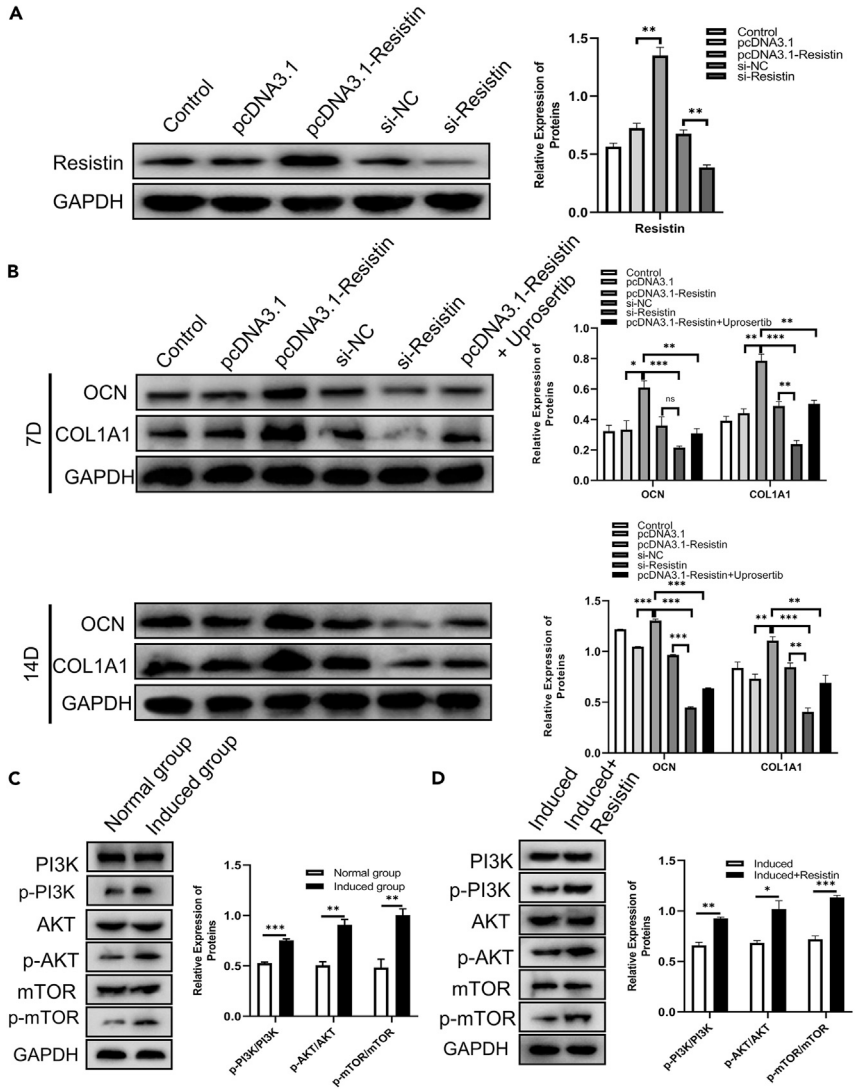

Figure 3. Resistin promotes OD by activating the PI3K/AKT/mTOR pathway

(A) Relative expression of resistin in different transfection groups.

(B) Relative expression of OCN, COL1A1 among different transfection groups at days 7 and 14.

(C) Relative expression levels of PI3K/AKT/mTOR pathway-related proteins.

(D) Relative expression levels of PI3K/AKT/mTOR pathway-related proteins after resistin treatment. Densitometry was performed using ImageJ software. Data were presented as means ± SEM. (*$p < 0.05$, **$p < 0.01$, and ***$p < 0.001$, one-way ANOVA or Student's *t* test).

were taken for histological and histomorphometric examinations. All rats survived well after surgery without developing any postoperative infection or death during the study. Micro-CT was performed to analyze the results of bone defect reconstruction. In the femoral defect group, severe cavitary bone loss was observed in the femoral condyle. In contrast, the resistin treatment group displayed gradual recovery of the defect area (Figures 6A and 6B). Quantitative analysis of bone microstructure parameters revealed that BMD, BV/TV, Tb.Th decreased significantly and Tb.Sp increased significantly in the femur defect group compared with the normal group. Meanwhile, resistin treatment significantly increased the BMD, BV/TV and Tb.Th and decreased the Tb.Sp, compared with the femoral defect group (Figure 6C). Exogenous resistin contributed significantly to OD and positively influenced new bone tissue formation.

H&E and Masson's staining were used to assess the repair of the femoral condyle. Figures 6D and 6E showed complete sagittal views of the femur and enlarged views of the defect. H&E staining

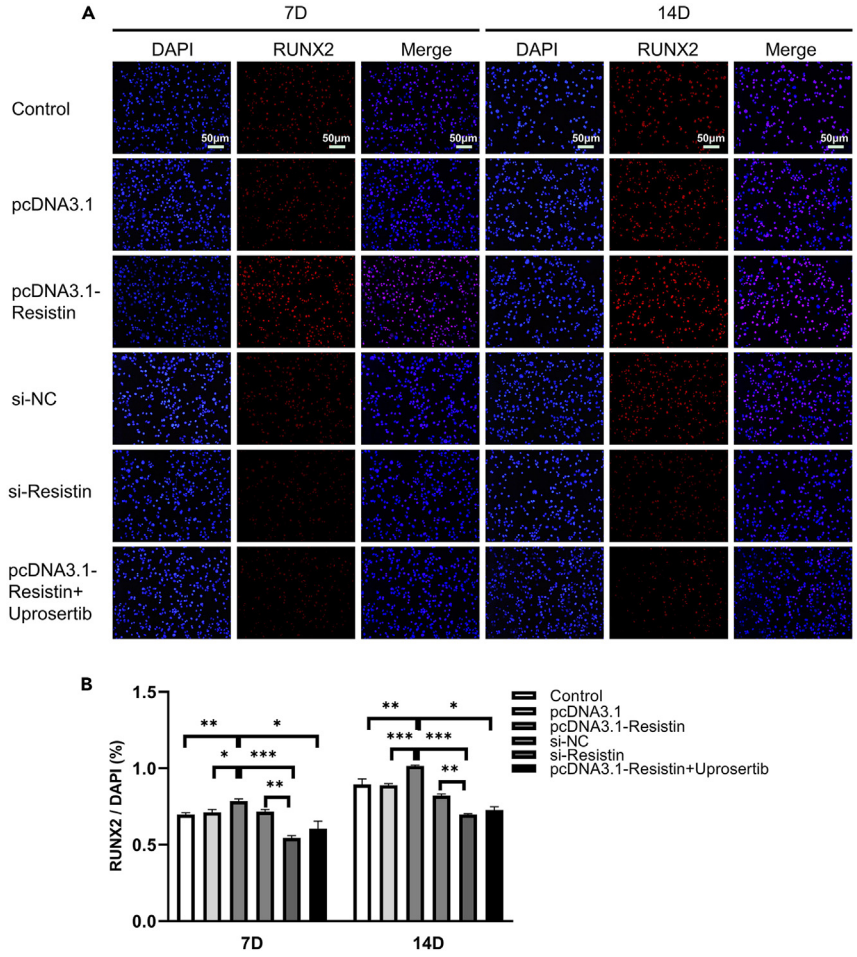

Figure 4. Representative images of immunofluorescence staining for RUNX2

(A) Fluorescence microscopy images among different transfection groups at days 7 and 14 (scale bar, 50μm).
(B) Quantification of RUNX2-positive cells per DAPI-positive nuclei. Positive cells were counted using ImageJ software. Data were presented as means ± SEM. (*p < 0.05, **p < 0.01, and ***p < 0.001, one-way ANOVA or Student's *t* test).

demonstrated that bone mineral density in the resistin treatment group was significantly higher than in the femoral defect group at 4 weeks post-surgery (Figure 6D). Masson's staining revealed that bone formation, consisting of blue and red cancellous bone, markedly increased around the femoral condyle defect, indicating increased calcification and new bone tissue remodeling (Figure 6E). The above results suggested that resistin displayed a favorable ability in pro-osteogenic differentiation and promoted rat bone defect healing.

In addition, RUNX2, COL1A1 and OCN immunohistochemical staining demonstrated osteoblasts' status, revealing resistin's influence on OD of BMSCs (Figure 6F). Moreover, the resistin treatment group showed stronger immunohistochemical signal and osteogenic properties than the femoral defect group. The semi-quantitative results aligned with the immunohistological staining results (Figures 6G–6I).

Furthermore, the immunofluorescence intensity of resistin and TAZ protein expression in the resistin treatment group, as shown by immunofluorescent experiments, was higher than that in the femoral defect group at 4 weeks after injury (Figures 7A and 7B). The semi-quantitative results shown in Figures 7C and 7D were consistent with the immunofluorescence results. Animal experiments confirmed that injection of resistin could upregulate TAZ, promoting OD of BMSCs.

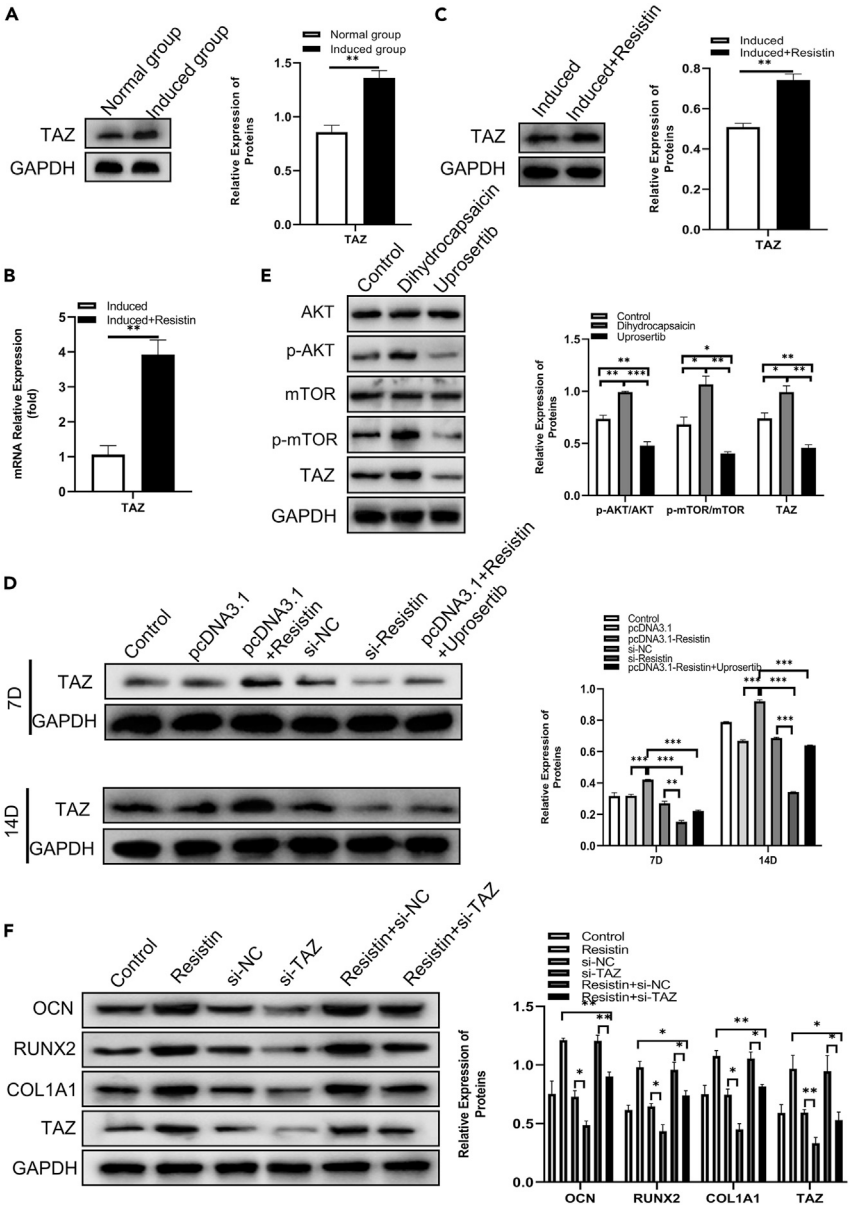

Figure 5. Resistin promoted OD via up-regulating TAZ *in vitro*

(A) Relative protein levels of TAZ.

(B) Resistin significantly increased the TAZ mRNA expression.

(C) Resistin significantly increased the TAZ protein expression.

(D) Relative expression of TAZ among different transfection groups at day 7 and 14.

(E) PI3K/AKT/mTOR pathway regulated the TAZ protein expression.

(F) TAZ knockdown markedly decreased the expression of OD related proteins (RUNX2, OCN, and COL1A1).

Densitometry was performed using ImageJ software. Data were presented as means ± SEM. (*$p < 0.05$, **$p < 0.01$, and ***$p < 0.001$, one-way ANOVA or Student's *t* test).

DISCUSSION

Bone defect repair follows a series of orchestrated biological events, including osteogenesis, osteoclastogenesis, and matrix mineralization.[26,27] Further insights into the formation and function of osteoblasts may lead to new directions for therapeutic targets for bone defect regeneration.[28] Osteoblasts are derived from mesenchymal stem cells, and osteogenic differentiation involves numerous molecular mechanisms and factors.[29] Therefore, studying the factors impacting on OD of BMSCs would significantly contribute to

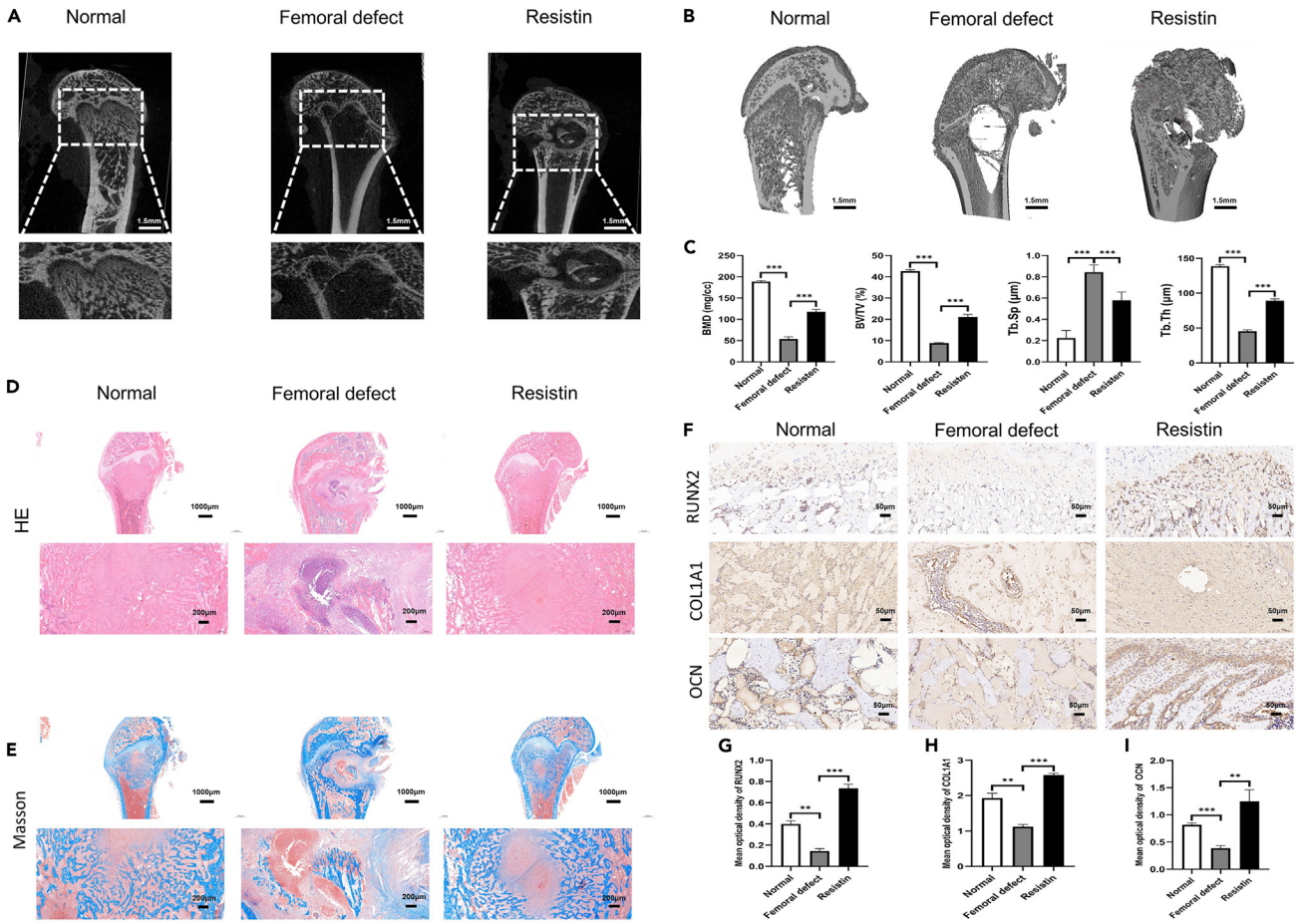

Figure 6. Resistin enhanced bone healing of femoral condyle defect

(A) Two dimensional (2D) reconstruction and partial magnification of femoral condyle defect at 4 weeks after surgery (scale bar, 1.5mm).

(B)Three dimensional (3D) reconstruction of femoral condyle defect at 4 weeks after surgery (scale bar, 1.5mm).

(C) Quantitative analysis of bone microstructure parameters such as bone mineral density (BMD), bone volume/tissue volume (BV/TV), trabecular separation (Tb.Sp), and trabecular thickness (Tb.Th).

(D) H&E stain and partial magnification (scale bar, 1000μm; magnification scale bar, 200μm).

(E) Masson's staining and partial magnification (scale bar, 1000μm; magnification scale bar, 200μm).

(F) Immunohistochemical staining for osteogenic markers COL1A1 and OCN (scale bar, 50μm).

(G–I) Semi-quantitative of immunohistochemistry for COL1A1 and OCN. The optical density values were detected by ImageJ software. Data were presented as means ± SEM. (**$p < 0.01$, and ***$p < 0.001$, Student's *t* test).

developing novel agents for bone defects. PI3K/AKT/mTOR has been generally recognized as an essential signaling pathway in regulating OD and has become a focus of research in the field of bone defects.[17–20] Adipocytokines resistin has been shown to participate in PI3K/AKT/mTOR pathway to regulate the initiation and progression of various diseases and have promising therapeutic potential in many diseased conditions.[21–23,29] However, the precise mechanism of resistin in bone defects has not been clearly elucidated. In this study, we demonstrated that resistin targeted TAZ to promote OD of BMSCs, and this effect was likely mediated by activation of the PI3K/Akt/mTOR pathway (Figure 8).

During the process of OD, COLIA1, RUNX2, SP7, and OCN are osteogenic marker genes at different stages.[28,30] In our *in vitro* research, resistin treatment significantly affected the mRNA and protein expression of RUNX2, OCN, and COl1A1 and promoted OD. For *in vivo* experiments, exogenous resistin enhanced bone healing of femoral condyle defect. Moreover, the resistin group showed higher protein expression of COL1A1 and OCN and more robust osteogenic properties. Thommesen et al. have previously shown that resistin stimulates the proliferation and differentiation of osteoblasts and osteoclasts and plays a role in regulating bone remodeling.[31] Therefore, resistin may represent a novel therapeutic approach to enhancing bone healing.

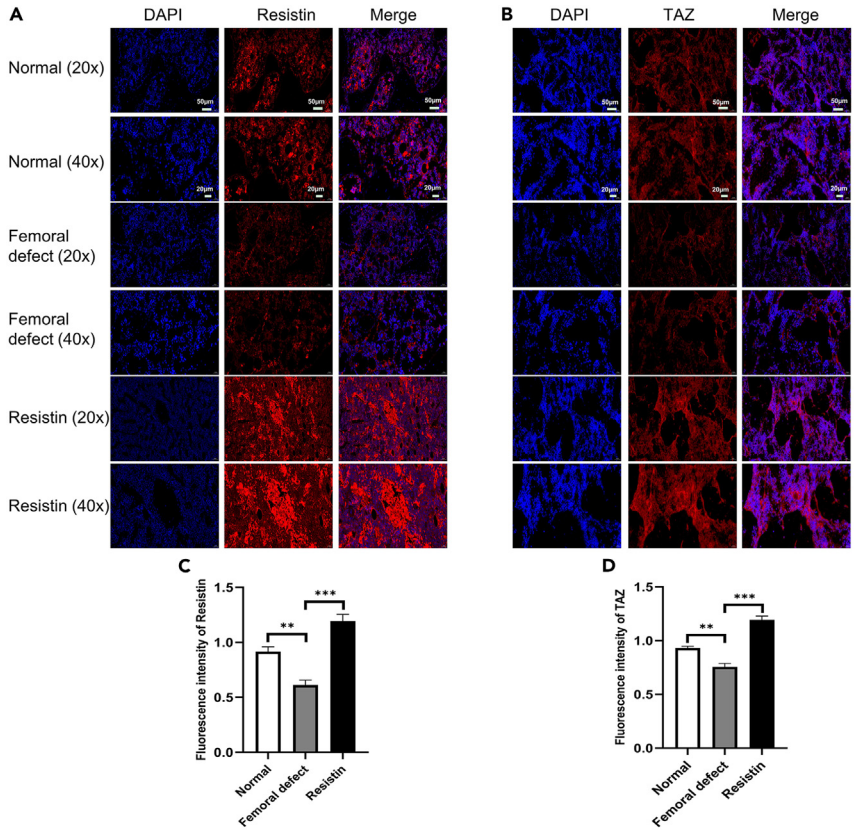

Figure 7. Resistin promoted OD via up-regulating TAZ *in vivo*

(A) Immunofluorescence images for resistin (20× magnification, scale bar, 50μm; 40× magnification, scale bar, 20μm).
(B) Immunofluorescence images for TAZ (20× magnification, scale bar, 50μm; 40× magnification, scale bar, 20μm).
(C and D) Semi-quantitative of immunofluorescence for resistin and TAZ. The fluorescence intensity was quantified using ImageJ software. Data were presented as means ± SEM. (**$p < 0.01$, and ***$p < 0.001$, Student's *t* test).

The specific signaling pathway mechanisms remain to be further explored. However, it has been shown that resistin overexpression can enhance the OD process. PI3K/AKT pathway has been considered a potential therapeutic target for bone defects therapy.[32] This pathway regulates multiple cellular functions, including proliferation, migration, autophagy, and metabolism.[33] Under normal conditions, the PI3K/AKT/mTOR pathway has been reported to selectively affect the physiological functions of osteoblasts and osteoclasts. Furthermore, during oxidative stress, the extent of oxidative damage is mitigated by acting on its downstream targets, including glycogen synthase kinase 3 beta and forkhead box O.[34] Other signaling pathways, including Wnt/β-catenin, Notch, and Bone morphogenic protein, are also implicated in regulating the OD of BMSCs.[35–37]

Previous studies revealed that resistin promoted VEGF-A-dependent angiogenesis of human chondrosarcoma cells via activating PI3K/AKT signaling pathway.[38] In this study, we demonstrated that PI3K/AKT/mTOR inhibitors suppressed the expression of resistin-induced osteogenic biomarkers. We found that PI3K and AKT phosphorylation was increased when cells were incubated with resistin. Next, BMSCs were co-transfected with uprosertib with pcDNA3.1-resistin to assess whether up-regulated resistin induced OD could be reversed by inhibiting PI3K/AKT/mTOR pathway. Moreover, WB and immunofluorescence assays indicated that inhibition of PI3K/AKT/mTOR could diminish OD induced by pcdna3.1-resistin. These findings suggest that PI3K/AKT/mTOR pathway is involved in the osteogenic effects mediated by resistin.

TAZ plays a critical role in the fate of multipotent stem cells and has been demonstrated to be a transcriptional modulator during osteoblast development and skeletogenesis.[39] Activating TAZ promoted the OD of stem cells.[40] Moreover, previous studies revealed a strong correlation between expression levels of TAZ and resistin in adipocytes.[19] Eugene Lee et al. investigated the changes in signaling pathways via RNA-seq gene analysis in rat bone defect models and found that osteogenesis and angiogenesis in stem cells were

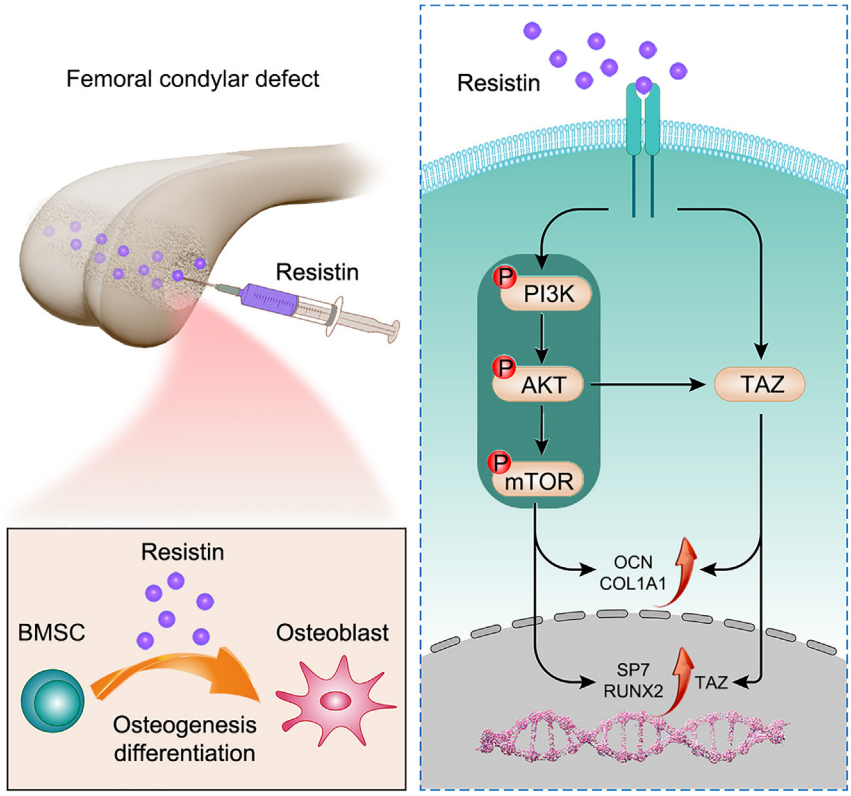

Figure 8. Schematic illustration of the proposed mechanism

enhanced by increasing TAZ expression.[41] In this study, we confirmed that resistin regulated the OD of BMSCs through TAZ activation. *In vivo*, resistin treatment could upregulate the expression of TAZ and osteogenic markers. *In vitro*, TAZ knockdown neutralized the influence of resistin overexpression on OD markers. Therefore, our results indicated that resistin affected OD by activating the TAZ signaling pathway. It was important to note that PI3K/AKT/mTOR pathway regulated the expression of TAZ and its inhibitors blocked resistin induced TAZ upregulation. This might be identified as a potential regulatory network.

In summary, our results highlighted new insight into resistin functions during OD. The mechanism of OD induced by resistin may be correlated with the activation of PI3K/AKT/mTOR signaling pathway, and the induction was attenuated by treatment with PI3K/AKT/mTOR inhibitor, implying a potential role for resistin in the pathogenesis of bone defects. In addition, we proposed that resistin promoted OD by targeting TAZ. These findings support targeting resistin/TAZ as a promising therapeutic strategy for bone defect regeneration.

Limitations of the study

In this article, some limitations exist in our study and should be noted. Firstly, although we identified that resistin targeted TAZ to induce OD through PI3K/AKT/mTOR pathway, the crosstalk with other signaling pathways cannot be ruled out, and the interaction between resistin and the OD-related genes remains to be further revealed. We next sought to explore other possible pathways, including Wnt/β-catenin pathway[42,43] and MAPK pathway,[44,45] and carry out relevant clinical studies. Secondly, bone defect remodeling is a dynamic process involving osteogenesis (bone formation) and osteoclastogenesis (bone resorption). Further studies are needed to characterize the role of resistin in osteoclastogenesis.

STAR★METHODS

Detailed methods are provided in the online version of this paper and include the following:

- KEY RESOURCES TABLE

ACKNOWLEDGMENTS

This study was supported by Changzhou Sci &Tech Program (Grant No. CJ20220120 and CJ20210104), Qinghai Province Health System Guidance Plan Project (2022-wjzdx-106), Funding from Young Talent Development Plan of Changzhou Health commission (CZQM2020059), and Changzhou High-Level Medical Talents Training Project (2022CZBJ059 and 2022CZBJ061). The funding sources had no role in data collection, analysis, interpretation, or reporting.

AUTHOR CONTRIBUTIONS

Conceptualization, J.J.S., Z.T.Y., and X.D.Z.; Methodology, J.J.S., Z.T.Y., C.W.X., J.J.Z., and J.H.G; Investigation, J.J.S., C.W.X., J.H.G., and C.L.Y.; Writing – Original Draft, J.J.S. and Z.T.Y.; Writing – Review and Editing, J.J.S. and X.D.Z.; Funding Acquisition, X.D.Z.; Resources, J.J.S., Y.H., and X.D.Z.; Supervision, X.D.Z., C.L.Y., and Y.H.

DECLARATION OF INTERESTS

The authors declare no competing interests.

INCLUSION AND DIVERSITY

We support inclusive, diverse, and equitable conduct of research.

Received: January 12, 2023
Revised: May 6, 2023
Accepted: May 30, 2023
Published: June 7, 2023

REFERENCES

1. Li, J.J., Dunstan, C.R., Entezari, A., Li, Q., Steck, R., Saifzadeh, S., Sadeghpour, A., Field, J.R., Akey, A., Vielreicher, M., et al. (2019). A novel bone substitute with high bioactivity, strength, and porosity for repairing large and load-bearing bone defects. Adv. Healthc. Mater. *8*, e1801298. https://doi.org/10.1002/adhm.201801298.

2. Liu, Y., Wang, R., Chen, S., Xu, Z., Wang, Q., Yuan, P., Zhou, Y., Zhang, Y., and Chen, J. (2020). Heparan sulfate loaded polycaprolactone-hydroxyapatite scaffolds with 3D printing for bone defect repair. Int. J. Biol. Macromol. *148*, 153–162. https://doi.org/10.1016/j.ijbiomac.2020.01.109.

3. Hak, D.J., Fitzpatrick, D., Bishop, J.A., Marsh, J.L., Tilp, S., Schnettler, R., Simpson, H., and Alt, V. (2014). Delayed union and nonunions: epidemiology, clinical issues, and financial aspects. Injury *45*, S3–S7. https://doi.org/10.1016/j.injury.2014.04.002.

4. Li, W., Liu, Y., Zhang, P., Tang, Y., Zhou, M., Jiang, W., Zhang, X., Wu, G., and Zhou, Y. (2018). Tissue-engineered bone immobilized with human adipose stem cells-derived exosomes promotes bone regeneration. ACS Appl. Mater. Interfaces *10*, 5240–5254. https://doi.org/10.1021/acsami.7b17620.

5. Ueno, M., Lo, C.W., Barati, D., Conrad, B., Lin, T., Kohno, Y., Utsunomiya, T., Zhang, N., Maruyama, M., Rhee, C., et al. (2020). Interleukin-4 overexpressing mesenchymal stem cells within gelatin-based microribbon hydrogels enhance bone healing in a murine long bone critical-size defect model. J. Biomed. Mater. Res. *108*, 2240–2250. https://doi.org/10.1002/jbm.a.36982.

6. Pittenger, M.F., Mackay, A.M., Beck, S.C., Jaiswal, R.K., Douglas, R., Mosca, J.D.,

Moorman, M.A., Simonetti, D.W., Craig, S., and Marshak, D.R. (1999). Multilineage potential of adult human mesenchymal stem cells. Science *284*, 143–147. https://doi.org/10.1126/science.284.5411.143.

7. Bianco, P., Riminucci, M., Gronthos, S., and Robey, P.G. (2001). Bone marrow stromal stem cells: nature, biology, and potential applications. Stem Cell. *19*, 180–192. https://doi.org/10.1634/stemcells.19-3-180.

8. Au, P., Tam, J., Fukumura, D., and Jain, R.K. (2008). Bone marrow-derived mesenchymal stem cells facilitate engineering of long-lasting functional vasculature. Blood *111*, 4551–4558. https://doi.org/10.1182/blood-2007-10-118273.

9. Yu, C., Chen, L., Zhou, W., Hu, L., Xie, X., Lin, Z., Panayi, A.C., Zhan, X., Tao, R., Mi, B., and Liu, G. (2022). Injectable bacteria-sensitive hydrogel promotes repair of infected fractures via sustained release of mirna antagonist. ACS Appl. Mater. Interfaces *14*, 34427–34442. https://doi.org/10.1021/acsami.2c08491.

10. Wang, Y., Yuan, M., Guo, Q.Y., Lu, S.B., and Peng, J. (2015). Mesenchymal stem cells for treating articular cartilage defects and osteoarthritis. Cell Transplant. *24*, 1661–1678. https://doi.org/10.3727/096368914x683485.

11. Zhao, B., Peng, Q., Poon, E.H.L., Chen, F., Zhou, R., Shang, G., Wang, D., Xu, Y., Wang, R., and Qi, S. (2021). Leonurine promotes the osteoblast differentiation of rat bmscs by activation of autophagy via the PI3K/Akt/mTOR pathway. Front. Bioeng. Biotechnol. *9*, 615191. https://doi.org/10.3389/fbioe.2021.615191.

12. Tanaka, Y., Sonoda, S., Yamaza, H., Murata, S., Nishida, K., Hama, S., Kyumoto-Nakamura, Y., Uehara, N., Nonaka, K., Kukita, T., and Yamaza, T. (2018). Suppression of AKT-mTOR signal pathway enhances osteogenic/dentinogenic capacity of stem cells from apical papilla. Stem Cell Res. Ther. *9*, 334. https://doi.org/10.1186/s13287-018-1077-9.

13. Zhao, X., Sun, W., Guo, B., and Cui, L. (2022). Circular RNA BIRC6 depletion promotes osteogenic differentiation of periodontal ligament stem cells via the miR-543/PTEN/PI3K/AKT/mTOR signaling pathway in the inflammatory microenvironment. Stem Cell Res. Ther. *13*, 417. https://doi.org/10.1186/s13287-022-03093-7.

14. Shen, Y.S., Chen, X.J., Wuri, S.N., Yang, F., Pang, F.X., Xu, L.L., He, W., and Wei, Q.S. (2020). Polydatin improves osteogenic differentiation of human bone mesenchymal stem cells by stimulating TAZ expression via BMP2-Wnt/β-catenin signaling pathway. Stem Cell Res. Ther. *11*, 204. https://doi.org/10.1186/s13287-020-01705-8.

15. Zhu, Y., Wu, Y., Cheng, J., Wang, Q., Li, Z., Wang, Y., Wang, D., Wang, H., Zhang, W., Ye, J., et al. (2018). Pharmacological activation of TAZ enhances osteogenic differentiation and bone formation of adipose-derived stem cells. Stem Cell Res. Ther. *9*, 53. https://doi.org/10.1186/s13287-018-0799-z.

16. Patel, L., Buckels, A.C., Kinghorn, I.J., Murdock, P.R., Holbrook, J.D., Plumpton, C., Macphee, C.H., and Smith, S.A. (2003). Resistin is expressed in human macrophages and directly regulated by PPAR gamma activators. Biochem. Biophys. Res. Commun. *300*, 472–476. https://doi.org/10.1016/s0006-291x(02)02841-3.

17. Zhou, X., Xi, K., Bian, J., Li, Z., Wu, L., Tang, J., Xiong, C., Yu, Z., Zhang, J., Gu, Y., Huang, Y., Cai, F., and Chen, L. (2023). Injectable engineered micro/nano-complexes trigger the reprogramming of bone immune epigenetics. Chem. Eng. J. *462*, 142158. https://doi.org/10.1016/j.cej.2023.142158.

18. Jamaluddin, M.S., Weakley, S.M., Yao, Q., and Chen, C. (2012). Resistin: functional roles and therapeutic considerations for cardiovascular disease. Br. J. Pharmacol. *165*, 622–632. https://doi.org/10.1111/j.1476-5381.2011.01369.x.

19. Gao, Y., Chen, X., He, Q., Gimple, R.C., Liao, Y., Wang, L., Wu, R., Xie, Q., Rich, J.N., Shen, K., and Yuan, Z. (2020). Adipocytes promote breast tumorigenesis through TAZ-dependent secretion of Resistin. Proc. Natl. Acad. Sci. USA *117*, 33295–33304. https://doi.org/10.1073/pnas.2005950117.

20. Li, J., Jiang, M., Yu, Z., Xiong, C., Pan, J., Cai, Z., Xu, N., Zhou, X., Huang, Y., and Yang, Z. (2022). Artemisinin relieves osteoarthritis by activating mitochondrial autophagy through reducing TNFSF11 expression and inhibiting PI3K/AKT/mTOR signaling in cartilage. Cell. Mol. Biol. Lett. *27*, 62. https://doi.org/10.1186/s11658-022-00365-1.

21. Kim, H.J., Lee, Y.S., Won, E.H., Chang, I.H., Kim, T.H., Park, E.S., Kim, M.K., Kim, W., and Myung, S.C. (2011). Expression of resistin in the prostate and its stimulatory effect on prostate cancer cell proliferation. BJU Int. *108*, E77–E83. https://doi.org/10.1111/j.1464-410X.2010.09813.x.

22. Pang, L., Zhang, Y., Yu, Y., and Zhang, S. (2013). Resistin promotes the expression of vascular endothelial growth factor in ovary carcinoma cells. Int. J. Mol. Sci. *14*, 9751–9766. https://doi.org/10.3390/ijms14059751.

23. Pardo, F., Subiabre, M., Fuentes, G., Toledo, F., Silva, L., Villalobos-Labra, R., and Sobrevia, L. (2019). Altered foetoplacental vascular endothelial signalling to insulin in diabesity. Mol. Aspects Med. *66*, 40–48. https://doi.org/10.1016/j.mam.2019.02.003.

24. Li, L., Wang, Y., Wang, Z., Xue, D., Dai, C., Gao, X., Ma, J., Hang, K., and Pan, Z. (2022). Knockdown of FOXA1 enhances the osteogenic differentiation of human bone marrow mesenchymal stem cells partly via activation of the ERK1/2 signalling pathway. Stem Cell Res. Ther. *13*, 456. https://doi.org/10.1186/s13287-022-03133-2.

25. Zhang, Y., Gu, X., Li, D., Cai, L., and Xu, Q. (2019). METTL3 regulates osteoblast differentiation and inflammatory response via smad signaling and MAPK signaling. Int. J. Mol. Sci. *21*, 199. https://doi.org/10.3390/ijms21010199.

26. Xu, Z., He, J., Zhou, X., Zhang, Y., Huang, Y., Xu, N., and Yang, H. (2020). Down-regulation of LECT2 promotes osteogenic differentiation of MSCs via activating Wnt/β-catenin pathway. Biomed. Pharmacother. *130*, 110593. https://doi.org/10.1016/j.biopha.2020.110593.

27. Huang, C.C., Kang, M., Lu, Y., Shirazi, S., Diaz, J.I., Cooper, L.F., Gajendrareddy, P., and Ravindran, S. (2020). Functionally engineered extracellular vesicles improve bone regeneration. Acta Biomater. *109*, 182–194. https://doi.org/10.1016/j.actbio.2020.04.017.

28. Gao, Y., Patil, S., and Jia, J. (2021). The development of molecular biology of osteoporosis. Int. J. Mol. Sci. *22*, 8182. https://doi.org/10.3390/ijms22158182.

29. Muruganandan, S., Ionescu, A.M., and Sinal, C.J. (2020). At the crossroads of the adipocyte and osteoclast differentiation programs: future therapeutic perspectives. Int. J. Mol. Sci. *21*, 2277. https://doi.org/10.3390/ijms21072277.

30. Komori, T. (2020). Molecular mechanism of RUNX2-dependent bone development. Mol. Cells *43*, 168–175. https://doi.org/10.14348/molcells.2019.0244.

31. Thommesen, L., Stunes, A.K., Monjo, M., Grøsvik, K., Tamburstuen, M.V., Kjøbli, E., Lyngstadaas, S.P., Reseland, J.E., and Syversen, U. (2006). Expression and regulation of resistin in osteoblasts and osteoclasts indicate a role in bone metabolism. J. Cell. Biochem. *99*, 824–834. https://doi.org/10.1002/jcb.20915.

32. Cui, H., Han, G., Sun, B., Fang, X., Dai, X., Zhou, S., Mao, H., and Wang, B. (2020). Activating PIK3CA mutation promotes osteogenesis of bone marrow mesenchymal stem cells in macrodactyly. Cell Death Dis. *11*, 505. https://doi.org/10.1038/s41419-020-2723-6.

33. Wu, C., Qiu, S., Liu, P., Ge, Y., and Gao, X. (2018). Rhizoma Amorphophalli inhibits TNBC cell proliferation, migration, invasion and metastasis through the PI3K/Akt/mTOR pathway. J. Ethnopharmacol. *211*, 89–100. https://doi.org/10.1016/j.jep.2017.09.033.

34. Wang, L., Wang, L., Shi, X., and Xu, S. (2020). Chlorpyrifos induces the apoptosis and necroptosis of L8824 cells through the ROS/PTEN/PI3K/AKT axis. J. Hazard Mater. *398*, 122905. https://doi.org/10.1016/j.jhazmat.2020.122905.

35. Zhao, Y., Richardson, K., Yang, R., Bousraou, Z., Lee, Y.K., Fasciano, S., and Wang, S. (2022). Notch signaling and fluid shear stress in regulating osteogenic differentiation. Front. Bioeng. Biotechnol. *10*, 1007430. https://doi.org/10.3389/fbioe.2022.1007430.

36. Bharadwaz, A., and Jayasuriya, A.C. (2021). Osteogenic differentiation cues of the bone morphogenetic protein-9 (BMP-9) and its recent advances in bone tissue regeneration. Mater. Sci. Eng. C Mater. Biol. Appl. *120*, 111748. https://doi.org/10.1016/j.msec.2020.111748.

37. Chen, X.J., Shen, Y.S., He, M.C., Yang, F., Yang, P., Pang, F.X., He, W., Cao, Y.M., and Wei, Q.S. (2019). Polydatin promotes the osteogenic differentiation of human bone mesenchymal stem cells by activating the BMP2-Wnt/β-catenin signaling pathway. Biomed. Pharmacother. *112*, 108746. https://doi.org/10.1016/j.biopha.2019.108746.

38. Chen, S.S., Tang, C.H., Chie, M.J., Tsai, C.H., Fong, Y.C., Lu, Y.C., Chen, W.C., Lai, C.T., Wei, C.Y., Tai, H.C., et al. (2019). Resistin facilitates VEGF-A-dependent angiogenesis by inhibiting miR-16-5p in human chondrosarcoma cells. Cell Death Dis. *10*, 31. https://doi.org/10.1038/s41419-018-1241-2.

39. Byun, M.R., Hwang, J.H., Kim, A.R., Kim, K.M., Hwang, E.S., Yaffe, M.B., and Hong, J.H. (2014). Canonical Wnt signalling activates TAZ through PP1A during osteogenic differentiation. Cell Death Differ. *21*, 854–863. https://doi.org/10.1038/cdd.2014.8.

40. La Noce, M., Stellavato, A., Vassallo, V., Cammarota, M., Laino, L., Desiderio, V., Del Vecchio, V., Nicoletti, G.F., Tirino, V., Papaccio, G., et al. (2021). Hyaluronan-based gel promotes human dental pulp stem cells bone differentiation by activating YAP/TAZ pathway. Cells *10*, 2899. https://doi.org/10.3390/cells10112899.

41. Lee, E., Ko, J.Y., Kim, J., Park, J.W., Lee, S., and Im, G.I. (2019). Osteogenesis and angiogenesis are simultaneously enhanced in BMP2-/VEGF-transfected adipose stem cells through activation of the YAP/TAZ signaling pathway. Biomater. Sci. *7*, 4588–4602. https://doi.org/10.1039/c9bm01037h.

42. Xiao, F., Shi, J., Zhang, X., Hu, M., Chen, K., Shen, C., Chen, X., Guo, Y., and Li, Y. (2023). Gadolinium-doped whitlockite/chitosan composite scaffolds with osteogenic activity for bone defect treatment: in vitro and in vivo evaluations. Front. Bioeng. Biotechnol. *11*, 1071692. https://doi.org/10.3389/fbioe.2023.1071692.

43. Zhang, M., Gao, Y., Li, Q., Cao, H., Yang, J., Cai, X., and Xiao, J. (2022). Downregulation of DNA methyltransferase-3a ameliorates the osteogenic differentiation ability of adipose-derived stem cells in diabetic osteoporosis via Wnt/β-catenin signaling pathway. Stem Cell Res. Ther. *13*, 397. https://doi.org/10.1186/s13287-022-03088-4.

44. Zhang, Y.L., Liu, F., Li, Z.B., He, X.T., Li, X., Wu, R.X., Sun, H.H., Ge, S.H., Chen, F.M., and An, Y. (2022). Metformin combats high glucose-induced damage to the osteogenic differentiation of human periodontal ligament stem cells via inhibition of the NPR3-mediated MAPK pathway. Stem Cell Res. Ther. *13*, 305. https://doi.org/10.1186/s13287-022-02992-z.

45. Kim, H., Oh, N., Kwon, M., Kwon, O.H., Ku, S., Seo, J., and Roh, S. (2022). Exopolysaccharide of Enterococcus faecium L15 promotes the osteogenic differentiation of human dental pulp stem cells via p38 MAPK pathway. Stem Cell Res. Ther. *13*, 446. https://doi.org/10.1186/s13287-022-03151-0.

46. Wang, N., Li, Y., Li, Z., Ma, J., Wu, X., Pan, R., Wang, Y., Gao, L., Bao, X., and Xue, P. (2019). IRS-1 targets TAZ to inhibit adipogenesis of rat bone marrow mesenchymal stem cells through PI3K-Akt and MEK-ERK pathways. Eur. J. Pharmacol. *849*, 11–21. https://doi.org/10.1016/j.ejphar.2019.01.064.

47. Hara, K., Hellem, E., Yamada, S., Sariibrahimoglu, K., Mølster, A., Gjerdet, N.R., Hellem, S., Mustafa, K., and Yassin, M.A. (2022). Efficacy of treating segmental bone defects through endochondral ossification: 3D printed designs and bone metabolic activities. Mater. Today. Bio *14*, 100237. https://doi.org/10.1016/j.mtbio.2022.100237.

48. Yamada, K., Uchiyama, A., Uehara, A., Perera, B., Ogino, S., Yokoyama, Y., Takeuchi, Y., Udey, M.C., Ishikawa, O., and Motegi, S.I. (2016). MFG-E8 drives melanoma growth by stimulating mesenchymal stromal cell-induced angiogenesis and M2 polarization of tumor-associated macrophages. Cancer Res. *76*, 4283–4292. https://doi.org/10.1158/0008-5472.can-15-2812.

STAR★METHODS

KEY RESOURCES TABLE

REAGENT or RESOURCE	SOURCE	IDENTIFIER
Antibodies		
RUNX2	Abcam	ab76956; AB_1565955; ab236639; AB_2937078
OCN	Santa Cruz	sc-390877; AB_2937079
SP7	Abcam	ab209484; AB_2892207
COL1A1	Santa Cruz	sc-293182; AB_2797597
resistin	Absin	abs120209; AB_2937080
TAZ	Abcam	ab224239; AB_2889852
PI3K	Abcam	ab151549; AB_151549
p-PI3K	Abcam	ab182651; AB_2756407
AKT	Abcam	ab179463; AB_2810977
p-AKT	Abcam	ab81283; AB_2224551
mTOR	Abcam	ab32028; AB_881283
p-mTOR	Abcam	ab109268; AB_10888105
GAPDH	Abcam	ab8245; AB_2107448
Chemicals, peptides, and recombinant proteins		
Akt inhibitor	MedChemExpress	S80052; 1047634-65-0
dihydrocapsaicin	Absin	abs819594; 19408-84-5
Resistin	Sigma-Aldrich	SRP4561
Critical commercial assays		
ALP assay kit	AnaSpec	N/A
flow cytometry	Beckman Coulter	FC500
Experimental models: Organisms/strains		
male SD rats	Changzhou Cavens Experimental Animal Co., Ltd	N/A
Oligonucleotides		
RUNX2 Forward (5′-3′): CGCCTCACAAACAACCACAG	Invitrogen	N/A
RUNX2 Reverse (5′-3′): AATGACTCGGTTGGTCTCGG	Invitrogen	N/A
OCN Forward (5′-3′): CACCACCGTTTAGGGCATGT	Invitrogen	N/A
OCN Reverse (5′-3′): CTTTCGAGGCAGAGAGAGGG	Invitrogen	N/A
SP7 Forward (5′-3′): TCTAGGATTGGATCTGAGTGAGCC	Invitrogen	N/A
SP7 Reverse (5′-3′): CATAGTGAGCTTCTTCCTGGGG	Invitrogen	N/A
COL1A1 Forward (5′-3′): GAGACAGGCGAACAAGGTGA	Invitrogen	N/A
COL1A1 Reverse (5′-3′): GGGAGACCGTTGAGTCCATC	Invitrogen	N/A

(*Continued on next page*)

Continued

REAGENT or RESOURCE	SOURCE	IDENTIFIER
Resistin Forward (5′-3′): GCTGCTGCCAACTGTCCTAA	Invitrogen	N/A
Resistin Reverse (5′-3′): AAGAAGCGGGGTTAATGGGC	Invitrogen	N/A
TAZ Forward (5′-3′): TTCTGAGTTCCTGCGCTTCA	Invitrogen	N/A
TAZ Reverse (5′-3′): AGGGTGGACTGTTAGGGAGG	Invitrogen	N/A
PI3K Forward (5′-3′): GGATATGAAGGGAGCCCCAGA	Invitrogen	N/A
PI3K Reverse (5′-3′): GACGCTGAGGAAGGGTCATTT	Invitrogen	N/A
AKT Forward (5′-3′): ATAACGGACTTCGGGCTGTG	Invitrogen	N/A
AKT Reverse (5′-3′): CCTGGTTGTAGAAGGGCAGG	Invitrogen	N/A
mTOR Forward (5′-3′): GCAATGGGCACGAGTTTGTT	Invitrogen	N/A
mTOR Reverse (5′-3′): AGTGTGTTCACCAGGCCAAA	Invitrogen	N/A
GAPDH Forward (5′-3′): TCTCTGCTCCTCCCTGTTCT	Invitrogen	N/A
GAPDH Reverse (5′-3′): ATCCGTTCACACCGACCTTC	Invitrogen	N/A
siRNA targeting sequence: siResistin-1: CAGCAAGAAGAUCAAUCAATT	TsingkeBiotechnologyCo.,Ltd.	N/A
siRNA targeting sequence: siResistin-2: UUGAUUGAUCUUCUUGCUGTT	TsingkeBiotechnologyCo.,Ltd.	N/A
siRNA targeting sequence: siTAZ-1: AGAUGGUGUCUAUCAGAAATT	TsingkeBiotechnologyCo.,Ltd.	N/A
siRNA targeting sequence: siTAZ-2: UUUCUGAUAGACACCAUCUTT	TsingkeBiotechnologyCo.,Ltd.	N/A
Recombinant DNA		
Resistin pcDNA3.1 plasmid	This paper	N/A
Software and algorithms		
Image J	Image J	Image J (RRID:SCR_003070)
GraphPad Prism 9.0	GraphPad Software Inc.	GraphPad Prism (RRID:SCR_002798)
Adobe Photoshop CS6	Adobe	Adobe Photoshop (RRID:SCR_014199)

RESOURCE AVAILABILITY

Lead contact

Further information and requests for resources and reagents should be directed to and will be fulfilled by the lead contact, Xindie Zhou (xindiezhou@163.com).

Materials availability

This study did not generate new unique reagents and all materials in this study are commercially available.

Data and code availability

- Data: All data reported in this paper will be shared by the lead contact upon request.

- Code: This paper does not report original code.
- Additional information: Any additional information required to reanalyze the data reported in this paper is available from the lead contact upon reasonable request.

EXPERIMENTAL MODEL AND STUDY PARTICIPANT DETAILS

Isolation and culture of BMSCs

According to previous studies, Sprague Dawley (SD) rats were used for subsequent animal experiments.[46,47] After euthanizing with carbon dioxide asphyxiation, bilateral femurs were harvested under aseptic conditions. All animal procedures were approved by the Animal Experiment Ethics Committee of the affiliated Changzhou NO.2 People's Hospital of Nanjing Medical University (Changzhou, China) and conformed to the Guide for the Care and Use of Laboratory Animals (US National Institutes of Health). Bone marrow was flushed with sterile Dulbecco modified Eagle medium (DMEM/F12, ThermoFisher Scientific, MA, USA). Bone marrow irrigating solution was centrifuged at 5000 rpm for 5 minutes and then placed in DMEM/F12 medium with 10% fetal bovine serum and 1% penicillin/streptomycin, then incubated at 37°C in a 5% CO_2 incubator for 48 hours. Subsequently, non-adherent cells were discarded, and adherent cells were cultured until 80% confluency. These subcultured cells were designated as the first passage (P1), and P3 was used for subsequent experiments.

Establishment of rat femur defect model

Thirty male SD rats (age: 6–8 weeks, weight: 230–300 g) were purchased from Changzhou Cavens Experimental Animal Co., Ltd. In this study, rats were randomly divided into three groups: normal group (sham-operated group; 0.9% saline treatment; n = 10), femoral defect group (operated group; 0.9% saline treatment; n = 10), and resistin group (operated group; resistin treatment; n = 10). The treatment was continued once weekly for 4 weeks. A rat femoral condyle bone defect model was used to evaluate the bone repair capability of resistin *in vivo*. The rats were first immobilized after the intraperitoneal injection of 2% pentobarbital sodium salt solution (2 mL/kg). After anesthesia and routine preparation, a sagittal midline incision was performed on the lateral aspect of the left hind limb. The femoral condyles were exposed, followed by blunt dissection of the muscles and periosteum. A bone defect (3 mm in diameter and 3 mm in depth) was then created on the femur using a low-speed drill. The surgical area was rinsed constantly with sterile saline solution to act as a coolant and to remove bone debris. Finally, the incision was sutured, and penicillin was injected intraperitoneally to prevent infection.

METHOD DETAILS

Flow cytometry

MSC marker CD44 and negative marker CD11b were identified using flow cytometry.[48] According to the manufacturer's protocol, cells (100μL, 1×10^6/mL) were incubated with antibodies against CD44 and CD11b (BD Biosciences, CA, USA) for 30 minutes and sorted by flow cytometry (FC500, Beckman Coulter, CA, USA).

Alizarin red staining

Cells were stained with alizarin red after 14 days of incubation in an osteogenic induction medium containing β-glycerophosphate and ascorbic acid (Sigma-Aldrich, MO, USA). The medium was removed, followed by rinsing in PBS and fixation in 4% paraformaldehyde for 30 minutes. After washing, alizarin red staining solution (ScienCell, CA, USA) was added and incubated for 20 minutes to determine calcium deposition. Staining was visualized using an optical microscope.

Alkaline phosphatase (ALP) activity measurement

BMSCs were collected and lysed after 14 days of culturing with normal and osteogenic media. ALP activity in BMSCs lysates was determined following the instructions of the ALP assay kit (AnaSpec, CA, USA). Finally, the absorbance was measured using a microplate reader (Multiskan FC, ThermoFisher Scientific).

Cell transfection

For alteration expression of resistin and TAZ, Lipofectamine 2000 (Invitrogen, CA, USA) was used for transfection according to the manufacturer's instructions after cells reached 80% confluence. Co-transfections

were performed using AKT inhibitor GSK2141795 (uprosertib, MedChemExpress, USA) with pcDNA3.1-resistin to verify the interaction between resistin and PI3K/AKT/mTOR signaling pathway.

Real-time quantitative PCR

After 14 days of osteogenic induction, total RNA was extracted from BMSCs using Trizol reagent (Invitrogen). NanoDrop 2000 (ThermoFisher Scientific) was used to measure RNA concentrations and RNA purity. RNA was reverse transcribed according to the reverse transcription kit's instructions (GeneCopoeia, MD, USA). The mRNA expression of target genes was measured using specific primers via real-time PCR. Relative gene expression was calculated using the $2^{-\Delta\Delta Ct}$ method, with GAPDH as the internal reference. Primers for RT-PCR were purchased from Invitrogen (Shanghai, China) and described in table below.

Primer sequences

Genes	Forward sequence (5′-3′)	Reverse sequence (5′-3′)
RUNX2	CGCCTCACAAACAACCACAG	AATGACTCGGTTGGTCTCGG
OCN	CACCACCGTTTAGGGCATGT	CTTTCGAGGCAGAGAGAGGG
SP7	TCTAGGATTGGATCTGAGTGAGCC	CATAGTGAGCTTCTTCCTGGGG
COL1A1	GAGACAGGCGAACAAGGTGA	GGGAGACCGTTGAGTCCATC
Resistin	GCTGCTGCCAACTGTCCTAA	AAGAAGCGGGGTTAATGGGC
TAZ	TTCTGAGTTCCTGCGCTTCA	AGGGTGGACTGTTAGGGAGG
PI3K	GGATATGAAGGGAGCCCCAGA	GACGCTGAGGAAGGGTCATTT
AKT	ATAACGGACTTCGGGCTGTG	CCTGGTTGTAGAAGGGCAGG
mTOR	GCAATGGGCACGAGTTTGTT	AGTGTGTTCACCAGGCCAAA
GAPDH	TCTCTGCTCCTCCCTGTTCT	ATCCGTTCACACCGACCTTC

Western blot analysis

Total protein was extracted from BMSCs using RIPA lysis buffer. Protein concentrations of the samples were quantified using a bicinchoninic acid protein assay kit (ThermoFisher Scientific). Protein per sample was analyzed using electrophoresis on a 12% (w/v) sodium dodecyl sulfate-polyacrylamide gel electrophoresis. Then, the separated proteins were transferred onto polyvinylidene difluoride membranes, which were blocked with 5% (w/v) non-fat dry milk for 1 hour at 37°C. Thereafter, membranes were incubated with the specific primary antibodies overnight at 4°C, followed by incubation with secondary antibodies for 1 hour. After three 5-minute washes with TBST, the expressions of proteins were visualized using enhanced chemiluminescence. The antibodies were as follows: RUNX2 (ab76956, Abcam), OCN (sc-390877, Santa Cruz), SP7 (ab209484, Abcam), COL1A1 (sc-293182, Santa Cruz), resistin (abs120209, Absin), TAZ (ab224239, Abcam), PI3K (ab151549, Abcam), p-PI3K (ab182651, Abcam), AKT (ab179463, Abcam), p-AKT (ab81283, Abcam), mTOR (ab32028, Abcam), p-mTOR (ab109268, Abcam) and GAPDH (ab8245, Abcam). The protein bands were captured using the iBright™ FL1500 imaging system (ThermoFisher Scientific), and quantification was performed via densitometry using Image J software. GAPDH was used as the internal reference protein. The relative protein expression levels were shown as the value between the grayscale value of the target protein and the grayscale value of the internal reference protein.

Immunofluorescence

After two weeks of incubation, BMSCs were fixed with 4% paraformaldehyde for 20 minutes and permeabilized with 0.5% Triton X-100 for 20 minutes. Following blocking in 1% BSA for 30 minutes, samples were incubated with anti-RUNX2 primary antibody (ab76956, Abcam, 1:1000) overnight at 4 °C, and then fluorescent secondary antibody at room temperature for 1 hour. After three washes, the cells were stained with 4′,6-diamidino-2-phenylindole (DAPI) for 5 minutes. The stained nuclei were observed under a fluorescence microscope. Relative positive cell ratio was quantified by Image J software.

Micro-computed tomography (CT) analysis

After SD rats were sacrificed 4 weeks after surgery, the femur specimens were harvested and fixed in 10% formalin at 4°C for 24 hours. Micro-CT was used to analyze the femur specimens, and the scanner was set at 65 kV, 385 μA, and a resolution of 18.0 μm/pixel. After scanning, the 2D and 3D images were reconstructed

with NRecon software (v.1.6.8.0, SkyScan). The parameters, including bone mineral density (BMD), tissue volume (TV), bone volume (BV), bone volume/tissue volume (BV/TV), trabecular separation (Tb.Sp), and trabecular thickness (Tb.Th), of the interested region for each specimen were assessed using the CTAn software (v.1.12.0, Skyscan).

Histological analysis

The fixed femoral condyles were decalcified with 0.5 M EDTA at 4°C for 21 days. Then, samples were incubated in 10% formic acid solution at room temperature, dehydrated in an ethanol gradient, embedded in paraffin, and cut into 4 μm thick sections. Bone healing and regeneration were analyzed histologically with hematoxylin and eosin (H&E) staining and Masson staining. Briefly, all sections were deparaffinized with xylene and rehydrated in gradient ethanol. After, H&E staining (G1005, Servicebio, China) and Masson staining (G1006, Servicebio, China) were performed according to the manufacturer's protocols. Stained images were captured with a microscope imaging system.

Immunohistochemistry was performed to evaluate the expression of specific markers, including RUNX2, COL1A1 and OCN, in bone tissues. The sections were placed in the antigen repair solution (Sigma-Aldrich) to unmask the antigen. Then, sections were incubated overnight with the RUNX2 (ab236639, Abcam), COL1A1 (sc-293182, Santa Cruz) or OCN (sc-390877, Santa Cruz) primary antibody and subsequently incubated with secondary antibodies. Finally, immunoreaction was visualized with 3,3′-diaminobenzidine (DAKO) and lightly counter-stained with hematoxylin. The number of positive cells was quantified using ImageJ software. The average optical density inside cells was calculated using the Image J software. Furthermore, resistin and TAZ immunofluorescence were performed on tissue sections to evaluate the efficacy of bone repair. Primary antibodies used for immunofluorescence were resistin (abs120209, Absin) and TAZ (ab224239, Abcam). The fluorescence intensity was quantified using Image J software.

QUANTIFICATION AND STATISTICAL ANALYSIS

Ten mice per group were analyzed in the *in vivo* experiments, and all *in vitro* experiments were performed in triplicate. Five representative images of each group were selected and used for the semi-quantitative analysis of immunofluorescent/immunohistochemical staining. Data were presented as means and standard error mean. Differences between two groups were compared by the Student's *t* test and differences among three or more groups using one-way ANOVA. GraphPad Prism 9.0 (GraphPad Software Inc., USA) and SPSS 25.0 (SPSS Inc., USA) were used for statistical analysis. Stars indicated significance level: *$p < 0.05$, **$p < 0.01$, and ***$p < 0.001$.